URC97162

Multi-window Controllers for Autonomous Space Systems

B. J. Lurie and F. Y. Hadaegh
Jet Propulsion Laboratory
California Institute of technology
Pasadena, CA 91109

Abstract.

Multi-window controllers *[1,2]* select between elementary linear controllers using nonlinear windows based on the amplitude and frequency content of the feedback error. The controllers are relatively simple to implement and perform much better than linear controllers. The commanders for such controllers only order the destination point and are freed from generating the command time-profiles.

The robotic missions rely heavily on the tasks of acquisition and tracking. For autonomous and optimal control of the spacecraft, the control bandwidth must be larger while the feedback can (and, therefore, must) be reduced.. Combining linear compensators via multi-window nonlinear summer guarantees minimum phase character of the combined transfer function. It is shown that the solution may require using several parallel branches and windows, Several examples of multi-window nonlinear controller applications are presented.

1. Composite nonlinear controllers

R was demonstrated in [1-5] that some nonlinear controllers perform better than any linear controllers. Therefore, the optimal controller is, generally, nonlinear.

For a sufficiently small region in the state space, the nonlinear optimal controller can be approximated well by a linear controller. For the adjacent region, another linear controller can be designed that would be optimal over this region, and so on. Then a cental design problem arises as of how to integrate these locally-optimal linear controllers into a composite nonlinear controller, and in particular, how to provide smooth transitions between these linear laws when the time trajectory crosses the borders between these regions.

The transitions between the control modes can be defined by ***participation rules*** illustrated in Fig. 1. Over some transition interval of a variable or condition, the controller action is the sum of the actions of the adjacent regional control modes, and at the ends of the interval only one of the modes (or parameters, or actions) takes place. The linear transition rule Fig. l(a) can be expressed as

$$action = action_1(1 - k) + k \cdot action_2, \qquad (1)$$

where the scalar ***k is*** changing from O to 1 over the transition interval. A smoother rule of the modes' changing is illustrated in Fig. l(b). Commonly, the precise shape of the participation rules does not matter much as long as it is monotonic, not too steep, and not too shallow.

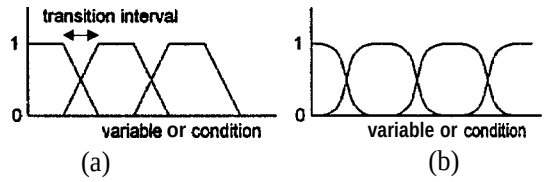

Fig. 1. Participation functions in composite controllers

The monotonic shape of the participation rules does not yet guarantee the smoothness of the transition. R is also required that the adjacent control laws mix well, i.e., the combined action of the adjacent controllers exceeds that of each individual controller. This is not always the case. For example, even if some residue that needs to be cleaned out can be removed by either an acid or a base, an acid and a base should not be used as a mixture with gradually changing content. For regulation of a reactive electrical current, a variable capacitor or a variable inductor can be used, but these elements should not be combined in series or parallel since they might produce resonances. A low-

pass link should not be mixed in parallel with a high-pros link or else notches and n.m.p.shift might result [2,5].
Fuzzy logic controllers break each smooth transition into several discrete steps. This increases the total number of regions with different control laws. Since these regions become small, fuzzy logic control can use low order regional control laws. Hence, fuzzy control design can be based on phase-plane partitions, and on passivity theory. However, in fuzzy logic controllers many variables need to be sensed and processed to define the boundaries of the regions.

What region size is optimal for composite controllers? There are two advantages of making the regions small. The first is that the control laws in the adjacent regions might become very similar which enables smooth transitions between them without taking special precautions. The second advantage is, because the linear controller can be of low order, the phase plane can be used for the controller analysis and design, and, as claimed by some of fuzzy logic advocates, the controllers can be designed even by those ignorant of control theory. However, when the number of the regions is large, the number of boundaries between them becomes very large. Correspondingly, the number of the decision making algorithms and instruments for changing between the control modes becomes very large. This complicates both the controller design and the designed controller.

On the other hand, higher order linear control laws can be made to remain nearly optimal over a much broader region than low-order laws. This reduces the number of the regions and the number of the boundaries between them thus making the designed controller much simpler. However, for the design of higher order regional control laws, not the phase plane but frequency domain methods should be used. The partition between the regions should be also somehow defined in the frequency domain. This approach requires caution and application of certain rules discussed in Chapter 4 to provide good blending of the regional control laws at the boundaries between the regions. Nevertheless, this approach is not difficult and leads to economical and nearly optimal controllers.

2. Multi-window control

In the following, we will consider a subset of the nonlinear controllers where the control law is dependent only on the amplitude of the error at the output of the feedback summer. The controller is composed of linear operators and non-dynamic (static) nonlinear functions determined by participation rules. It will be shown in examples and by ***some*** argumentation that such controllers provide nearly optimal performance for a wide variety of practical problems.

The sets of the error signals can be bounded by two-dimensional ***windows*** shown in Fig. 2(a). The windows divide the frequency spectrum (or, equivalently, time-response behavior) and the amplitude range. Within each window, some optimal linear operator (probably, of high order) is employed.

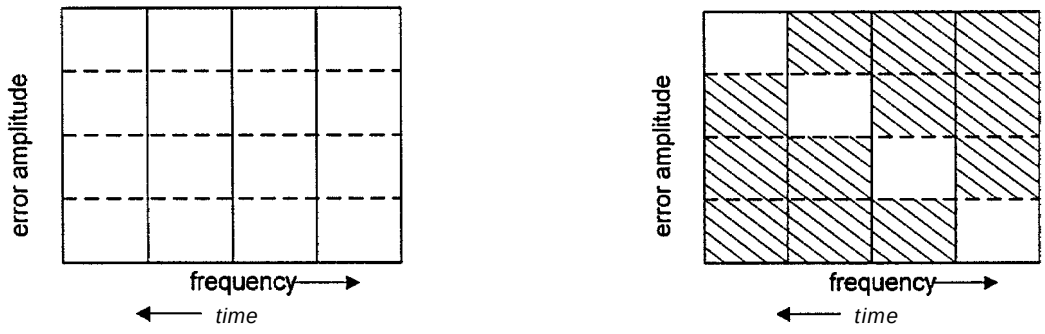

Fig. 2. The multi-window control concept: (a) the choice of the linear controller defined by the error amplitude and frequency content, (b) the linear controller is defined only by the error amplitude

When the amplitudes change, other windows become active and the control law changes. The amplitudes of different frequency components of the error define the composite control law.

The multiwindow nonlinear controller can be implemented as follows: the error is partitioned into components belonging to several windows, the components which belong to a window processed by the window linear operator, and the results combined by nonlinear functions implementing the appropriate participation law. This architecture is referred to as ***multi-window***, and a great number of useful nonlinear control schemes can be cast in this form.

In many practical cases, the correlation between the error's amplitude and the frequency content allows using only the diagonal windows as shown in Fig. 2(b). (The error amplitude can be linearly weighted.) The optimal linear controllers within each window can be designed using Bode integrals as the realizability limitation and the criterion for minimum phase behavior as the condition of smooth blending with the adjacent regions differing in frequency.

High-order linear regional controllers can be made nearly optimal not only within rather wide assigned windows, but also over some reasonably wide margins overlapping the adjacent windows, In this case, with relatively steep participation rules and narrow transition areas as illustrated in Fig, 3, the participation rules and the position of the borders between the windows become not critical.

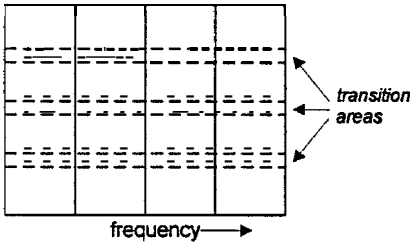

Fig. 3. Transition areas at the window borders

When the transition area is narrow (which often is the case), the transition is only required to be smooth. When the transition area is comparable to the area of the window, the transitional nonlinear control law must also be optimal. The transitional operators can be analyzed and synthesized using either the absolute stability approach or the describing function approach, using as the design constraints the Bode integrals.

The static nonlinearities used to implement the transition between the control modes lend themselves to realization using fuzzy rules. The nonlinearities are chosen (like saturation) such that sharp discontinuities are avoided.

Two-window compensators are widely employed (although not always optimized) in practical feedback systems, particularly, in anti-windup schemes, in acquisition and tracking systems, and in Nyquist-stable systems for provision of global and process stability.

The multiwindow compensator is a nonlinear dynamic compensator. And, vice versa, the NDC discussed in [2], whether they are made as a combination of parallel channels or as links with nonlinear local feedback, are multiwindow controllers. In [2], composite nonlinear controllers are studied as the means of providing global stability and process stability. In this paper, we concentrate on applications.

3. Windup, and anti-windup controllers

The overshoot in a system with saturation for the large amplitude input step can be excessive and persistent – this phenomenon is called ***windup. The*** windup can be many times longer than the overshoot in the linear mode of operation. Windup is caused by a combination of two factors: the error integration in the compensator and the actuator saturation. The saturation limits the return signal and therefore prevents the error signal accumulated in the compensator integrator from being compensated. During the initial period after the step command is applied, when the output is still low and the error is large, the compensator integrates the error. When the time comes at which this integrated error would be compensated by the return signal in the linear mode of operation, this does not happen for large commands, since the return signal is reduced by the actuator saturation. Then, it might take a long time for the feedback to compensate the integrated error. The error "hangs up", and only after some time, the output signal drops to the steady state value.

Using the DF concept, the qualitative explanation for the windup phenomenon goes as follows. Actuator saturation reduces the describing function loop gain thus shifting the equivalent crossover frequency down in frequency. The resulting overshoot is long, corresponding to this low crossover frequency. The value of the windup depends on the loop phase lag. When the phase stability margin is more than 70°, the windup is practically nonexistent, but it is large when the stability margin is 30° or smaller. The windup can be reduced or eliminated by employing nonlinear dynamic compensation.

Windup in *PID* system is commonly reduced or eliminated by placing a saturation in front or after the integrator, or resetting the integrator. A saturation link with different threshold is sometimes placed as well in front of P-term as shown in Fig. 4 thus making a three-window controller.

The diagram in Fig. 2 is somewhat ambiguous since it does not indicate whether the frequency selection or the amplitude selection is performed frost. Often a particular order is required. This order is different in the block diagrams in Fig. 5 which exemplifies two types of architectures for multi-window compensators.

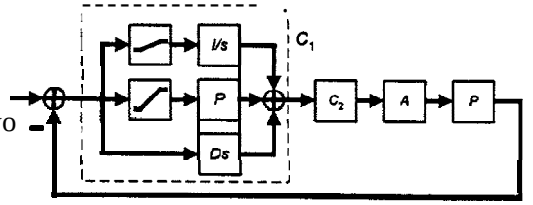

Fig. 4. Saturation in front of *I*- and P-paths.

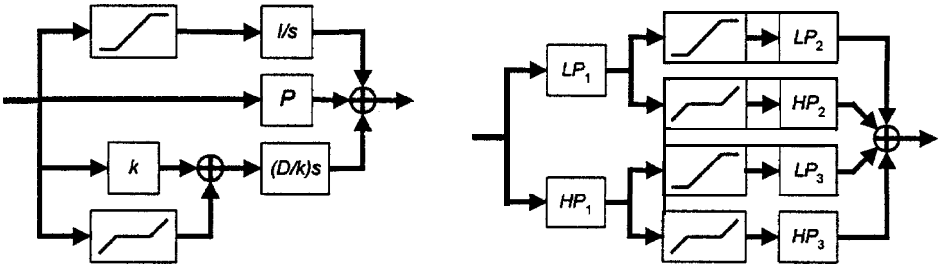

(a) (b)

Fig. 5. Multi-window compensators with parallel channels

Fig. 5(a) shows compensators with parallel channels. In such compensators, saturation links are commonly placed in the low-frequency channel since this channel's gain response dominates at lower frequencies. At large signal levels, the saturation link reduces the low-frequency gain and the phase lag of the compensator decreases thus reducing or eliminating windup. Placing a saturation link in front of the Z-path in *PID* controller commonly allows making small both the length and the height of the overshoot. In doing so, the value of the saturation threshold is not very critical. Placing a dead-zone element in front of the high-frequency channel with $k < 1$, also reduces the phase lag at large signal amplitudes which helps to eliminate the windup and improve the transient response.

Also, the windows can be placed in the local feedback path of an amplifier in the compensator. The performance of such multiwindow controllers is at least as good as that of the parallel paths controllers, and in this case the design can be placed on firm foundation of Popov absolute stability criterion [2,3,5],

4. Acquisition and tracking

Acquisition and tracking systems, like those used in homing missiles, are designed to operate in two modes: acquisition mode when the error is large, and tracking mode when the error is small. An example of the acquisition/tracking type is a pointing control system for a spacecraft-mounted camera, in which a rapid retargeting maneuver is followed by a slow precise scanning pattern to form a mosaic image. Another example is clock acquisition in the phase-locked loops of telecommunication systems and frequency synthesizers. When the error signal is large, i.e. the system is in the acquisition regime, the controller should respond as rapidly as possible, i.e. the feedback bandwidth should be wide. In the acquisition mode it is not necessary however that the feedback be very large, since the error is big anyway. In contrast, in the tracking regime, the feedback bandwidth needs to be reduced to reduce the output effects of the sensor noise, but the value of the feedback should be made rather large to minimize the tracking error. The differing loop frequency responses for the two modes are depicted in Fig. 6.

While the determination of theoptimal frequency responses for the acquisition mode and for the tracking mode is straightforward, guaranteeing smooth transient responses during transition from acquisition to tracking is not trivial. The transition can generate large transients in the output and error signals. If the transients are excessively large, the target can be de-acquired.

The transition between the responses can be done by switching or, better, by using nonlinear windows: the small errors are directed to the tracking compensator, and the large errors directed into the acquisition compensator. When using the windows, special care must be taken to ensure that all intermediate combined frequency responses of the parallel channels are acceptable. Intermediate response might result in an unstable system, or in a system with small stability margins and, therefore, producing large amplitude transient responses.

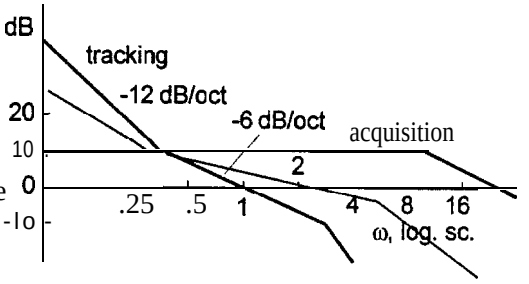

Fig. 6. Acquisition/tracking loop

As an example, let the total loop response be the weighted sum of the acquisition and tracking responses:

$$T = (1-k)T_{acq} + kT_{tr}, \qquad (2)$$

and suppose that k smoothly varies from O to 1 as the transition from acquisition mode to track mode occurs. For a certain value of k, the gains in the two paths are equal at the frequency f_1 indicated in Fig. 6. At this point the difference in phase between the two transfer fictions exceeds 180°, and the result is that a zero of the total transfer function T moves into the right half-plane ofs. The transient generated while the system remains in this state can be big and disruptive, even causing the target to be lost.

The conditions for the two parallel path transfer function $W_1 + W_2$ to become n.m.p. when each of the channels is m.p., is given in [2]. When the response is changing between two responses that, which combined, form n.p. lag that causes oscillation in the feedback loop – what happened? Qualitatively, we can describe the effect as follows. When one response dies down and the second response gradually rises to power, there is a time interval when they both are active, with the describing function k producing n.p. loop transfer describing function. When this time interval is long enough, a violent transient can occur that might lead to the target de-acquisition. For example, when the system in Fig. 5 with responses of Fig. 6 was modified so that the compensators are not switched instantly but their outputs combined via nonlinear windows, the overshoot in computer simulation reached 500%.

Therefore, when using two-window controllers with nonlinear blending of the linear controllers, the two compensator responses should not differ as much as those shown in Fig. 6. Hence, the two-window controller, although substantially better than a linear controller, still do not allow implementation of the best possible responses for acquisition and for tracking. This can be done with a three window controller using an intermediate frequency response during the transition which will look like the dotted line in Fig. 6.

5. Time-optimal control

Time-optimal control means changing the output variable between the commanded limits in minimum time, with limited force or power amplitude. For example, shifting a , mass with limited force amplitude in minimum time results in the force profile shown in Fig. 7. This control switches the force from positive to negative values at appropriate instants. The switching must occur at exactly right moments or else the final error will be large. When the plant is uncertain, the moments cannot be exactly calculated, and the open loop control entails considerable errors.

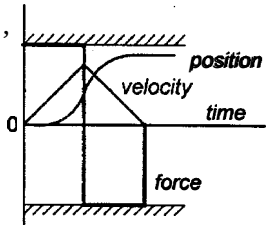

Fig. 7. Time-optimal control of a rigid plant position

When the time-optimal control has to be implemented closed loop-wise, it still should provide swift transitions from the maximum positive to maximum negative values, i.e. transitions very close to switching. The switching controller is a relay controller, i.e. a controller with infinite gain in the loop. An approximation to this controller is a controller with saturation and very large gain of linear links of the loop. The problem of designing such controller is therefore a feedback maximization problem while providing global stability and windup elimination. The solution to this problem also requires using an NDC, i.e. a multi-window controller as was shown in [4,5].

A reasonable complexity linear controller cannot provide time-optimal control. But a nonlinear, even a simple two-window controller, can be quite good. For most common problems, two windows suffice. However, when the transition between the modes must be very fast, or when the dynamic range is large, more windows may be necessary. For example, time-optimal precision pointing of space optical telecommunication systems with a huge *range* of error from acquisition to tracking would require more than two windows.

Example 1: Despin Control for S/C Booster Separation. The spacecraft booster is stabilized by spinning at 85 RPM. After separation from the booster, the spacecraft shown in Fig. 8(a) is despun by yo-yo to about 2 RPM, (The yo-yo is a weight at the end of a cable wrapped several times around the spacecraft. When the spacecraft is released from the booster rocket, the weight is also released and begins unwrapping the cable. When all the cable length is unwrapped, the cable is separated from the spacecraft, and the yo-yo takes away most of the rotation momentum.) The remaining spacecraft spin needs to be removed by fining thrusters. The spacecraft is unstable for spinning about z-axis since it is prolate, and the despin should be fast. Because of huge uncertainty in the initial conditions after the separation, with various positions and spin rates and different types of coupling between the axes, the controller design for the despin function must be made very robust, and at the same time, it must perform in a nearly time-optimal fashion. After the despin is complete, the controller must be changed to provide better control accuracy in the cruise mode.

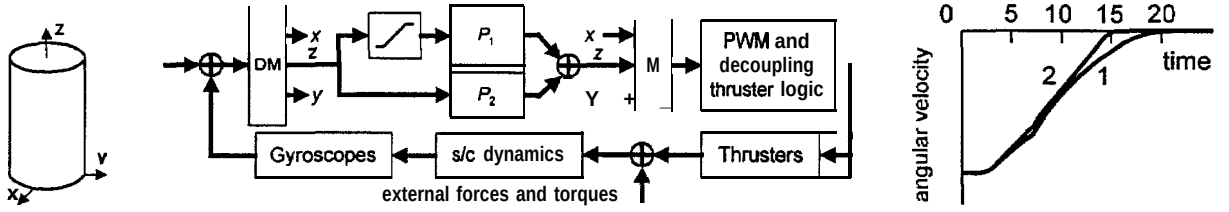

(a) (b) (c)

Fig. 8. A spacecraft (a) local frame coordinates, (b) attitude control system block diagram, (c) time-response of z-axis despinning

The controller shown in Fig. 8(b) uses pulse width modulated (PWM) thrusters. Since each thruster produces *x*-, y-, and z-torques, they are combined in pairs and decoupled by the thruster logic matrix. This renders the control of each axis independent to a certain extent. The problem is however complicated by coupling between the *x, y,* and *z*-rotations due to the spacecraft dynamics, including spinning of fuel and oxidizer, initially at the rate of the booster. Due to large plant uncertainty, despin was chosen to be proportional, providing large phase stability margin over the entire frequency range of possible plant uncertainty and x-, y-, and z-controllers coupling.

In the block-diagram, the demultiplexer DM separates vector into its components. The multiplexer M is doing the opposite. The compensators are independent for the x-, y-, and z-rotations, i.e., the controller matrix is diagonal.

When the controllers' gains were chosen such as to despin the s/c without substantial overshoot, the z-axis response was as shown in Fig, 8(c), curve 1. It is seen that the control is not time-optimal.

A better controller can be designed using fuzzy logic, with switching between different control laws depending on the variable values. Because of the complex spacecraft dynamics, there could be many ways to choose the switching conditions. However, the study of these options would be expensive and time consuming. Instead, a two-window nonlinear controller was designed which only changes the control law on the basis of the absolute value of the error in each channel. This was done by passing the errors via saturation-dead zone windows so that smooth transition between the control laws was provided. The resulting control law is nearly perfect for the despin function and as well for the cruise mode. The transient response for this controller is shown by the curve (2). The de-spin time was reduced by 20°/0.

The two-window controller performs better and is at the same time more robust than the original linear controller, with larger stability margins for large error mode when the cross-axis coupling is the largest.

This example shows that even for complicated plants with multi-channel coupled nonlinear feedback loops, a nonlinear two-window controller using only the error in individual channels for changing the control law provides nearly time-optimal performance, substantially better than that of linear controllers.

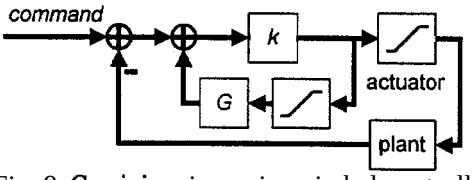

Fig. 9. Cassini main engine gimbal controller

Example 2. [n Cassini spacecraft, the main engine (thruster) is gimballed. The trajectory maneuvers can be performed by articulating the engine in *x*- and y-directions. The block diagram for the x-axis controller is shown in Fig. 9.

The error is processed by a two-window nonlinear controller which has a local feedback path comprising a saturation link and the guidance filter G. Small errors are multiplied by the transfer function $k/(1-G)$. Large errors are multiplied by k. Intermediate amplitude errors are processed by the nonlinear compensator which is an intermediate between the two linear compensators. The two-window controller is of the kind described in [2,3]. It eliminates the wind-up, allows for large disturbance rejection, and assures asymptotic global stability.

The Cassini attitude control employs thrusters (without PWM). The plant is close to a pure double integrator, although there may be flex modes at high frequencies. The thrusters are not throttled and not modulated, the torque is positive or negative some fixed value, or zero (similar to a 3-position relay.) These controllers also employ two-window nonlinear compensators.

Example 3. Temperature controller for the mirrors of the Narrow View Camera of Cassini spacecraft. The camera is a small telescope shown in Fig. 10(a). The primary and the secondary mirrors of the camera must be kept at approximately same temperature in order for the mirror surfaces to match each other, and the image in the focal plane to be clear. Fig. 11 shows Bode diagrams for three [parallel channel compensator. The low-frequency (LF) channel is preceded by a saturation element which constitute amplitude window for the feedback error. The transient response to a step input is shown in Fig. 12. The time-response of the heater power shows that the controller is nearly time-optimal. The controller was described in more detail in [1].

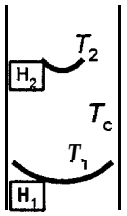

Fig. 10. Narrow Angle Camera

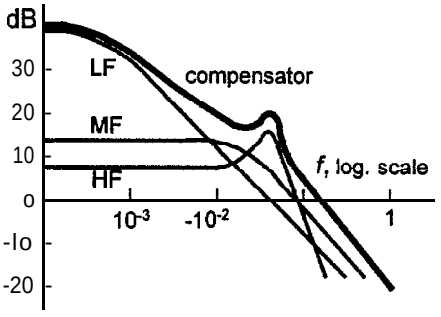

Fig. 11: Parallel-channel compensator responses

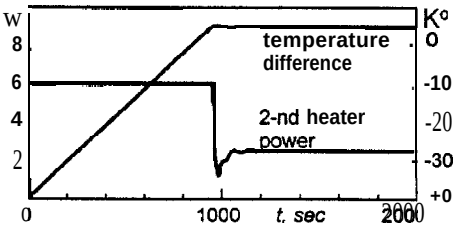

Fig. 12. Step response for thermal controller

Example 4. An tunnel-effect accelerometer [6] is shown in Fig. 13(a). The proof mass and the soft springs it is suspended on are etched of Silicon. The position of the proof mass is regulated by electrostatic forces between the proof mass and the upper and lower plates. The accelerometer uses tunnel effect sensor of the proof mass position. The voltage on the lower plate equals the voltage on the upper plate plus some bias. It can be shown that with proper bias voltage, the upper plate voltage is proportional to the measured acceleration.

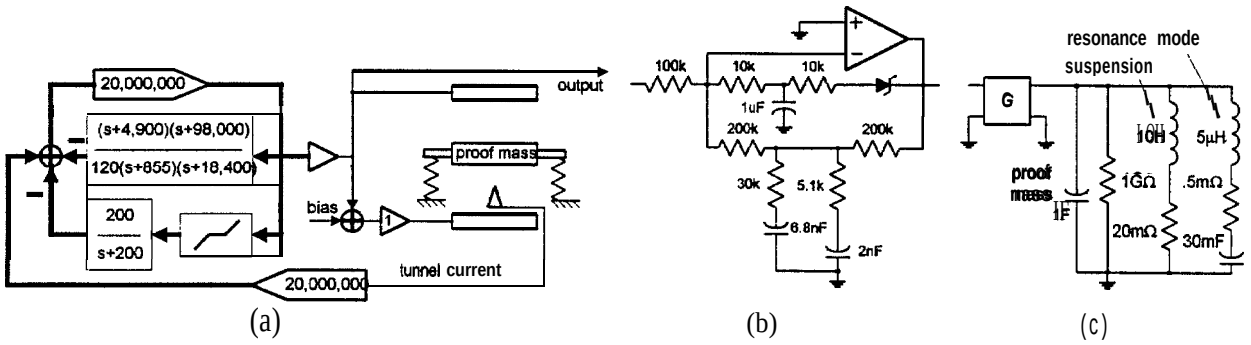

Fig. 13. Silicon accelerometer block diagram (a), compensator (b), and electrical analog plant model (c)

To achieve the desired accuracy, the feedback in the proof mass control loop must be larger than 100 dB at frequencies up to 5 Hz. The feedback crossover frequency f_b is limited by the dynamics (structural resonances) of the proof mass and suspension system to less than 3 kHz.

The tunnel current is the exponent of the inverse value of the tunnel effect gap. The normal value of the gap is approximately 6 Angstrom, but initially, the gap can be smaller, the tunnel current much larger, the derivative of it (the tunnel sensor sensitivity) also larger, and the loop gain bigger than nominal. The system global stability is provided by using a NDC with dead-zone in the local feedback path.

The mechanical plant might have some resonance modes with uncertain frequencies over 500 Hz. The quality factor of the resonances is not higher than 20, i.e. 26 dB.

The compensator is shown in Fig. 13(b). The dead-zone element was chosen non-symmetrical (a Zener diode) since the characteristic of the tunnel effect sensor is also non-symmetrical. For low level signals the Zener is not conducting, and the compensator response is determined by the lower feedback path. Two series RC circuits shunting the feedback path provide two leads giving sufficient phase stability margins over the range 200 to 3000 Hz. The Bode diagram and the Nyquist plot for signals of small amplitudes simulated in SPICE are shown in Fig. 13. When the signal is exceeding the Zener threshold, the diode opens and the upper feedback path, which is a low-pass, reduces the compensator gain at lower frequencies by approximately 30 dB. This gain reduction reduces the slope of the Bode diagram, substantially increases the phase stability margin at frequencies below 200 Hz, and improves the transient response of the closed loop which is important since the acquisition range of the tunnel effect sensor is very narrow, only about 15 Angstrom.

This controller provides global stability with the loop phase shift of π at frequencies where the loop gain is large, eliminates windup, reduces the overshoot, and increases the acquisition band of the tunneling condition. The tunnel effect is an exponential function, and if the feedback loop was initialized when the distance in the tunnel sensor gap was much smaller than normal, then, the loop gain is much larger, and the system would become unstable if it were not for the gain reduction by the NDC.

Example 5. A small parabolic antenna tracking the Earth is placed on Pathfinder Mars Lander. Two identical brushless motors with internal analog rate feedback loops articulate the antenna in two orthogonal directions. The motors are controlled by two independent identical SISO controllers.

The sampling frequency is 8 Hz. Were the delay caused only by the sampling, the crossover frequency would be $f_s/5 \approx$ 1.6 Hz. However, since the computer must handle not only the motor control loops but other higher priority tasks, there is an additional 500 msec delay caused by four real time interrupt (RTI) delays, 125 msec each. Also, due to limited bandwidth of the analog rate controllers for the motors (already designed), the motors have 50 msec delay. Since the total delay is not only 62.5 msec (of sampling) but 62.5 + 500 + 50 $\approx$ 600 msec, the realizable crossover frequency is lower in proportion to this delay, i.e. $f_b < 1.6.62.5/600 \approx$ O. 17 Hz.

The controller includes two cascaded linear links, $C_1 + 1$ and C_2. A saturation link placed in front of C_1 makes the transfer function of the compensator dependent on the signal level. When the signal level is below the saturation threshold, the compensator transfer fiction is $(C_1 + 1)C_2$. When the signal is high, the compensator transfer function reduces to C_2.

For small signal amplitudes, the compensator function is C = $(C_1 + 1)C_2$ where C_1 is a single-pole low pass filter Cl = 2.5/(0.0833 +s) and C_2 is a lead link, C_2 = (0.106 + s)/(2.23 + s). The asymptotic gain frequency responses of the compensator links are shown in Fig. 14. The digital compensator equations C_1 = (O. 15 + O. 15/z)/(1 - 0.99/z), C_2 = (0.9 - 0.8883 /z)/(1 - 0.75/2).

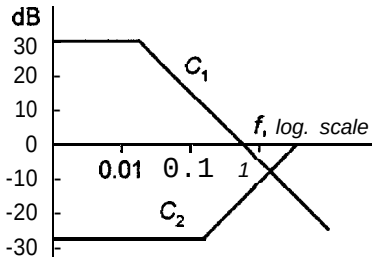

Fig. 14. Asymptotic Bode diagrams for compensators

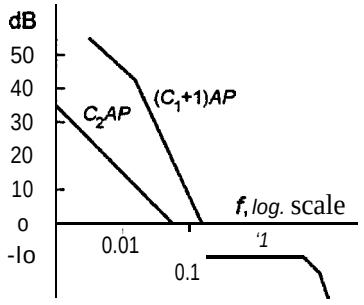

Fig. 15. Open loop asymptotic Bode diagrams of the compensators for small error (upper curve) and large error (lower curve)

The asymptotic loop gain frequency responses are shown in Fig. 15 for the case of both C_1 and C_2 operational, and for the case of C_1 = O (lower curve). The Bode step is very long because of the necessity to compensate for large time delay of up to 7 RTI, and to reduce or eliminate the overshoot,

The simplified feedback loop block diagram is shown in Fig. 16. The block diagram includes saturation in the higher gain, low frequency path; linear links C_1 and C_2; a scaling block that has saturation and a dead zone; the delay block; and the model of the plant (of the motor with its analog control electronics). The variable dur_out is the duration of the motor to be on during the sampling period of 125 msec. The motor is rate-stabilized by an analog loop with 30 msec rise-time. The motor transfer function is therefore that of an integrator (the angle of rotation is proportional of the time the motor is on) with an extra pole caused by the limited bandwidth of the analog rate loop.

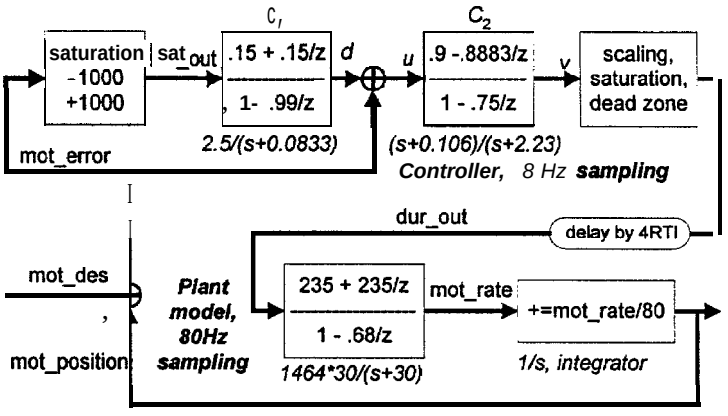

Fig. 16. Motor controller flow chart

Conclusion. Multiwindow controllers employed in space systems designed at JPL outperform conventional linear controllers and simplify the commanders.

We believe that such controllers should replace linear controllers in most of control systems, students must be taught that, generally, the controllers must be nonlinear, and newer control schemes should be compared to multiwindow controllers (instead of to linear controllers) to determine their advantages. (For example, it is shown in many examples that some fuzzy logic and neural network controllers perform substantially better than the best linear controllers, but comparisons to well designed multiwindow controllers are typically missing.)

Acknowledgment. This work was performed at the Jet Propulsion Laboratory, California Institute of Technology, under a contract with the National Aeronautics and Space Administration. The authors acknowledge contributions of Dr. P. Enright (who, in particular, designed the Cassini main engine articulation controller and the attitude thruster controller) and Drs. D. Bayard and M. Mesbahi for technical discussions.

References

1. P. J. Enright, F. Y. Hadaegh, B. J. Lurie, Nonlinear Multi-window Controllers. AIAA Guidance Navigation and Control Conference, July 29-31, 1996, San Diego, CA.
2, B. J. Lurie, P. J. Enright. *Classical* ***Feedback Control,*** manuscript, 1996.
3. B. J. Lurie, Absolutely Stable Feedback System with Dynamic Nonlinear Corrector. "Proc. IEEE", vol. 70, no. 8, 1982.
4. B. J. Lurie, Absolutely-Stable Nyquist-Stable Nonlinear Feedback System Design. "Intern. J. Control", vol. 40, no, 6, 1984.
5. B. J. Lurie, ***Feedback Maximization.*** Artech House, Dedham, MA: 1986.
6. B. P. Dolgin, F. T. Hartley, B. J. Lurie, P.M. Zavracky, Electrostatic Actuation of a Microgravity Accelerometer, 43rd National Symposium of American Vacuum Society, Microelectronical Mechanical Systems Topical Conference, Philadelphia, Pa 14-18 Oct. 1996.